phys. stat. sol. (b) 57, 157 (1973)

Subject classification: 13.2; 12.1; 21.1

Department of Physics, Brown University, Providence, Rhode Island

Uniaxial Stress Dependence of the Fermi Surface of Zinc[1])

By

I. I. GERSTEIN[2]) and C. ELBAUM

The effect of uniaxial stress on the areas of several orbits of the zinc Fermi surface have been studied by measuring the phase shifts of the magnetoacoustic quantum oscillations of ultrasonic attenuation. The orbits studied were the two third-zone electron orbits, i.e., the lens (ζ) and the needles (α), and four hole orbits on the second-zone monster, i.e., two horizontal arm orbits (β), with the magnetic field, $\boldsymbol{H}$, along $\langle 11\bar{2}0\rangle$ and $\langle 10\bar{1}0\rangle$, and two junction orbits (σ), with $\boldsymbol{H}$ along $\langle 11\bar{2}0\rangle$, and the bow-tie orbit (λ) with $\boldsymbol{H}$ along $\langle 10\bar{1}0\rangle$. Calculations of the stress dependence were carried out on the basis of a non-local pseudopotential model for the zinc Fermi surface and compared with the experimental results obtained. Good numerical agreement was thus obtained in half of the cases studied. Discrepancies of about a factor of two were found in the other cases, while the largest and smallest values of the stress derivatives (both measured and calculated) differed by as much as a factor of 100.

Der Einfluß einachsiger Spannung auf die Flächen verschiedener Bahnen der Fermiflächen von Zink wurden durch Messung der Phasenverschiebungen der magneto-akustischen Quantenoszillationen der Ultraschalldämpfung untersucht. Die untersuchten Bahnen waren die beiden Elektronenbahnen der dritten Zone, d. h. die Linse (ζ) und die Nadeln (α) und vier Löcherbahnen auf dem Monster der zweiten Zone, d. h. zwei Bahnen des horizontalen Arms (β) mit Magnetfeld $\boldsymbol{H}$ in Richtung $\langle 11\bar{2}0\rangle$ and $\langle 10\bar{1}0\rangle$, zwei Verbundbahnen ($\sigma$) mit $\boldsymbol{H}$ in Richtung $\langle 11\bar{2}0\rangle$ und die Schleifenbahn (λ) mit $\boldsymbol{H}$ in Richtung $\langle 10\bar{1}0\rangle$. Die Rechnung der Spannungsabhängigkeit wurde auf der Grundlage eines nicht-lokalen Pseudopotentialmodells für die Zink-Fermifläche durchgeführt und mit erhaltenen experimentellen Werten verglichen. In der Hälfte der untersuchten Fälle wurde gute numerische Übereinstimmung erhalten. Diskrepanzen bis zu einem Faktor zwei wurden in den anderen Fällen gefunden, während die größten und kleinsten Werte der Spannungskoeffizienten (sowohl gemessen als auch berechnet) sich um mehr als den Faktor 100 unterschieden.

1. Introduction

The Fermi surface of zinc has been extensively studied, both theoretically and experimentally. Linear and areal dimensions have been determined by a number of workers [1 to 6] and reasonable quantitative agreement with the nearly-free-electron (NFE) model has been found. Better models, which were obtained by fitting experimentally determined areas, were the local pseudopotential model of Harrison [7] and subsequently the non-local pseudopotential model of Stark and Falicov [8]. Measurements of linear dimensions [6] by the rf size effect gave a good confirmation of the latter model. Measurements have also been reported on the effect of hydrostatic pressure [9] and of alloying [10] on various smaller sections of the zinc Fermi surface. (The Fermi surface of zinc is shown

[1]) Research supported by the National Science Foundation and the Advanced Research Projects Agency. This article is based in part on the doctoral thesis of I. I. Gerstein.

[2]) Present address: Pratt and Whitney Co., Materials Engineering and Research Lab., Middletown, Connecticut 06457.

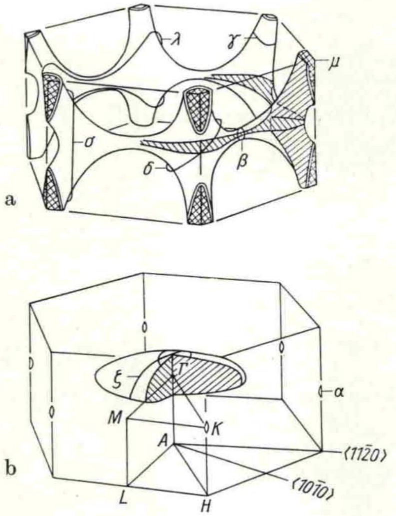

Fig. 1. The Fermi surface of zinc according to Gibbons and Falicov. a) First and second band of holes (first band "caps" are shown crosshatched). b) Third band of electrons. The capital letters designate symmetry points of the Brillouin zone and the small greek letters show the orbits discussed in the text

in Fig. 1, with the orbits discussed in the present work marked.) The most recent hydrostatic pressure work and the alloying experiments both show good agreement with the NFE model for the "needles" orbit (the third-zone electron section marked α in Fig. 1). Also studied in these experiments were the horizontal arms or waists (β) and the diagonal arms (γ) on the "monster", the hole segment in the second Brillouin zone. The results for these orbits were in no better than qualitative agreement with predictions based on both the NFE model and the local pseudopotential model.

The present work was undertaken to determine the effects of uniaxial stress on the Fermi surface of zinc. This was done by measuring the shift in phase of quantum oscillations in ultrasonic attenuation as stress was applied. The measurements on the needles were done with the stress in the hexad axis direction. The effects of stress in the basal plane were determined for the β orbit (in both the $\langle 10\bar{1}0\rangle$ and $\langle 11\bar{2}0\rangle$ directions), for two larger, more complex orbits on the monster σ and λ (referred to as the junction and the bow-tie sections respectively), and for another large orbit, ζ, on the third-zone electron lens. Theoretical predictions for the changes to be expected were obtained by introducing the lattice strains into the formalism of the Stark-Falicov non-local pseudopotential model [8].

In Section 2 the experimental apparatus and techniques are described. The theoretical calculations are discussed in Section 3. Section 4 contains the results both of the experiments and of the calculations. A summary of the results and conclusions is given in Section 5.

2. Experimental Apparatus and Techniques

The zinc crystals used in this work had residual resistivity ratios ($\varrho_{300\,°K}/\varrho_{4.2\,°K}$) of 6000 to 16000. The samples were rectangular parallelepipeds with the three sets of faces perpendicular to the three principal symmetry directions ($\langle 10\bar{1}0\rangle$, $\langle 11\bar{2}0\rangle$, and $\langle 0001\rangle$). The samples varied in their exact sizes, but a typical dimension was 1 cm.

The ultrasonic attenuation was measured by the conventional pulse-echo technique [11]. The frequency used was 90 MHz for wave propagation in the basal plane, and 30 HMz for propagation along the hexad axis. Longitudinal waves were used throughout, and the transducers were 30 MHz X-cut quartz. Magnetic fields of up to 80 kOe were generated by a superconducting solenoid, with a field homogeneity of approximately 5×10^{-5} over the volume of the sample.